PAPER

Dynamics of inertial particles under velocity resetting

Journal of Statistical Mechanics: Theory and Experiment
An IOP and SISSA journal

PAPER: Classical statistical mechanics, equilibrium and non-equilibrium

Dynamics of inertial particles under velocity resetting

Kristian Stølevik Olsen* **and Hartmut Löwen**

Institut für Theoretische Physik II—Weiche Materie,
Heinrich-Heine-Universität Düsseldorf, D-40225 Düsseldorf, Germany
E-mail: olsen@thphy.uni-duesseldorf.de

Received 24 January 2024
Accepted for publication 29 February 2024
Published 27 March 2024

Online at stacks.iop.org/JSTAT/2024/033210
https://doi.org/10.1088/1742-5468/ad319a

Abstract. We investigate stochastic resetting in coupled systems involving two degrees of freedom, where only one variable is reset. The resetting variable, which we think of as hidden, indirectly affects the remaining observable variable via correlations. We derive the Fourier–Laplace transforms of the observable variable's propagator and provide a recursive relation for all the moments, facilitating a comprehensive examination of the process. We apply this framework to inertial transport processes where we observe the particle position while the velocity is hidden and is being reset at a constant rate. We show that velocity resetting results in a linearly growing spatial mean squared displacement at later times, independently of reset-free dynamics, due to resetting-induced tempering of velocity correlations. General expressions for the effective diffusion and drift coefficients are derived as a function of the resetting rate. A non-trivial dependence on the rate may appear due to multiple timescales and crossovers in the reset-free dynamics. An extension that incorporates refractory periods after each reset is considered, where post-resetting pauses can lead to anomalous diffusive behavior. Our results are of relevance to a wide range of systems, such as inertial transport where the mechanical momentum is lost in collisions with the environment or the behavior of living organisms where stop-and-go locomotion with inertia is ubiquitous. Numerical simulations for underdamped Brownian motion and the random acceleration process confirm our findings.

Keywords: Brownian motion, diffusion, renewal processes

*Author to whom any correspondence should be addressed.

Contents

1. Introduction

Many processes in nature involve degrees of freedom that evolve in seemingly stochastic ways [1–3]. In many cases, large jumps in the values of an observed state variable can occur, which may drastically change the overall dynamics. Stochastic resetting is an example of large and sudden jumps where a degree of freedom is reset to its initial value at random times [4–6]. Over the past decade, stochastic resetting has garnered much attention in the non-equilibrium statistical physics community for multiple reasons. First, it has been shown to optimize the target search processes, with potential applications ranging from computer science to the understanding of animal foraging strategies [7–9]. Furthermore, resetting generates *non-equilibrium* steady states by trapping the system in a never-ending loop in the transient dynamical regime. Only recently have these non-equilibrium states been studied under the lens of stochastic thermodynamics, giving insights into exactly how far from thermal equilibrium such systems are [10–15]. The majority of past work is based on the dynamics and resetting of a single degree of freedom. In the presence of multiple state variables, with resetting only acting on a subset of these variables, a much richer phenomenology can occur. This paper studies

J. Stat. Mech. (2024) 033210

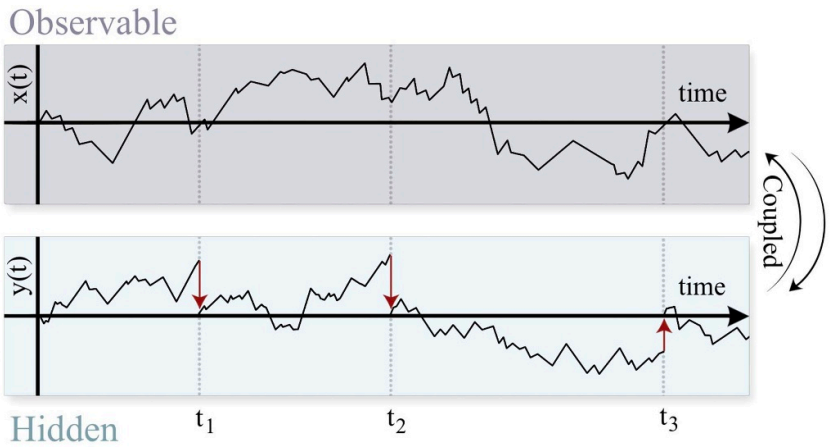

Figure 1. Sketch of the system under consideration. A set of coupled stochastic variables (x, y) where only y is being reset (partial resetting) at random times $\{t_i\}$. We consider a case where the reset variable is hidden from observations and infer indirect consequences of the resetting on the dynamics of the observable variable x.

such *partial resetting*[1] in a coupled two-dimensional system (figure 1), with a particular focus on the case of position and velocity as is pertinent to physics.

Partial resetting has only been studied in a handful of cases in the past, to the best of our knowledge. In dimensions higher than one, one can consider the resetting of only one spatial component [16]. For underdamped Brownian particles, the resetting of either the position alone or the simultaneous reset of position and velocity has been studied [17]. Similar types of partial resets have been considered for the random acceleration processes, where both the propagator and survival probabilities have been investigated [18, 19]. Since the position of a particle can be seen as the area under the velocity curve, connections between velocity resetting and large deviation theory can be made. In large deviation theory, one often studies time-additive observables such as the area under the curve, which have recently been studied under resetting [20–23]. Velocity resetting is also natural within active matter, where resetting schemes have recently been considered, where one can reset both the position and direction of motion, or only one of these variables [24–28]. Furthermore, the run-and-tumble motion is in itself a velocity resetting process [29–31]. Recently, a similar problem where an overdamped particle in a potential is driven by a resetting noise was investigated using Kesten variables, where both propagators and moments were studied [32].

While much has been known regarding the direct effect of resetting on a state variable, much less is known in general about the indirect effects of partial resetting in coupled systems. An example of this could be that one (or several) degrees of freedom are either not experimentally available or simply not of interest. If these unobserved, or

[1] One should note that the terminology *partial resetting* is sometimes also used for reset processes where $x \to ax$, with $a \in (0,1)$ the strength of the resetting. Here we use the phrasing *partial* in stead to refer to the resetting of parts of the set of degrees of freedom.

J. Stat. Mech. (2024) 033210

hidden, degrees of freedom undergo resetting, they may indirectly affect the observed degrees of freedom through cross-correlations. A situation where this can occur is in the underdamped dynamics of a Brownian particle. Collisions with the environment or with a substrate may induce a loss of mechanical momentum, effectively acting as a resetting of the velocity variable. Its position, however, remains unaffected by the resetting and only changes its dynamics indirectly through its coupling to velocity. This is different from the previous studies of resets in underdamped dynamics where only position was reset, or both variables reset simultaneously [17, 18].

Stochastic resetting of velocities can also be of relevance to various foraging strategies of animals and insects. An example is the intermittent stopping of flying foragers, such as bees in flowers, where the velocity is reset to zero but position remains unchanged. Similar behavior, referred to as stop-and-go locomotion, is ubiquitous in the behavior of macroscopic living organisms. Here, individuals intermittently stop their motion completely [33, 34], for example in order to save energy [35] or to scout for predators. This has, for example, been observed in fish motion [36], in chipmunk foraging strategies [37], and in lizards climbing trees [38]. Such macroscopic systems are, typically, also heavily prone to inertial effects, which the framework presented in this paper incorporates by default.

In this paper, we study the dynamics of a two-variable process where only one variable undergoes resetting. We consider one variable to be the observed variable, which does not undergo resets, whereas the other variable undergoes Poissonian resetting at a constant rate and is for brevity referred to as the hidden variable. We derive explicit expressions for the Fourier–Laplace transforms of the observed variables' propagator and derive from it a hierarchy of moments. We use this framework to study the dynamics of inertial particles when only the velocity is being reset. We show that when the velocity is reset to zero, at late times the mean squared displacement is always linear with an effective diffusivity that depends on the resetting rate. Extensions to the case where refractory periods are included after each reset are presented, wherein the late-time process may become anomalous if the refractory times are power-law distributed.

This paper is organized as follows. Section 2 discusses the propagator for two generic coupled variables when only one of them is being reset. Section 3 applies these results in the case of inertial transport processes, and discusses effective transport coefficients under velocity resetting. Section 4 extends these results in the case where refractory periods are included after each reset. Section 5 provides a concluding discussion and potential outlooks.

2. Propagators in coupled systems with resetting

For the sake of simplicity, we consider two coupled degrees of freedom (x, y), where we observe x, whereas the variable y experiences resets. Extensions to multiple variables are straightforward as long as all variables that undergo resetting do so simultaneously, in which case y may be seen as a collective variable. We denote the full propagator of the system in the presence of resetting by $p_r(x, y, t|x_0, y_0)$, where (x_0, y_0) are the initial conditions at $t = 0$. The starting point of our analysis is the well-known renewal

J. Stat. Mech. (2024) 033210

framework for resetting processes [6], which we augment to the present case of partial resetting. The last renewal equation can be used to express the propagator in terms of the propagator of the underlying, or reset-free, system $p_0(x,y,t|x_0,y_0)$ as follows:

$$p_r(x,y,t|x_0,y_0) = \mathrm{e}^{-rt}p_0(x,y,t|x_0,y_0) + r\int_0^t \mathrm{d}\tau \int \mathrm{d}x'\mathrm{d}y' p_r(x',y',t-\tau|x_0,y_0)\, p_0(x,y,\tau|x',y_0)\,\mathrm{e}^{-r\tau}. \quad (1)$$

Here, the intuition is the same as in most renewal processes; the first term corresponds to realizations of the system where no resetting occurs. These paths occur with probability e^{-rt}, and the system evolves with the $r=0$ propagator. The second term considers general trajectories (with resetting) up to the time of the last resetting $t-\tau$. The resetting occurs with probability $r\mathrm{d}\tau$. At this instant, the system is in some arbitrary state (x',y'). As only y is reset, the system proceeds to evolve toward (x,y) from the new initial condition (x',y_0). In this last time interval τ, there is no resetting, again taking place with probability $\mathrm{e}^{-r\tau}$.

Another item of note regarding equation (1) is the fact that all memory is deleted at the instance of reset, *except for the variable x*. Indeed, even if there were additional time dependencies coming from external effects, such as dynamical disorder from a changing environment or diffusion with a time-dependent drift, for example, even the environmental evolution must be reset for the full renewal structure assumed in equation (1) to be valid. This is simply due to the fact that the free propagator which links $(x',y_0)\to(x,y)$ over the duration $(t-\tau,t)$ in equation (1) only depends on the duration τ. Generally, time-heterogeneity can break the renewal structure one often desires while working with resetting processes. Often, it is assumed that any time-dependent parameters or annealed disorder is simultaneously reset with the system variables to make the system fully renewing [25, 39, 40]. In the case of an overdamped scaled Brownian motion, where the temperature either grows or decreases in time, *non-renewal* resetting has been studied recently, where the time dependence of the temperature is allowed to persist through a resetting event [41].

We are interested in the marginalized propagator of the observable variable x_t, which we denote:

$$\wp_r(x,t|x_0,y_0) \equiv \int \mathrm{d}y p_r(x,y,t|x_0,y_0) \quad (2)$$

and similarly for the process without resets. The indirect effect of resetting on the variable x can then be obtained by integrating over y in the above renewal equation:

$$\wp_r(x,t|x_0,y_0) = \mathrm{e}^{-rt}\wp_0(x,t|x_0,y_0) + r\int_0^t \mathrm{d}\tau e^{-r\tau}\int \mathrm{d}x'\wp_r(x',t-\tau|x_0,y_0)\,\wp_0(x,\tau|x',y_0). \quad (3)$$

To proceed, we restrict our attention to a class of spatially homogeneous systems, wherein the underlying $(r=0)$ propagator satisfies:

$$\wp_0(x,\tau|x',y_0)=\wp_0(x-x',\tau|y_0). \tag{4}$$

This casts the renewal equation of a convolution form, and we may readily apply a Fourier transform in space and a Laplace transform in time to solve the equation. We use the conventions:

$$\mathcal{L}_s[f(t)]\equiv\tilde{f}(s)=\int_0^\infty \mathrm{d}t e^{-st}f(t), \tag{5}$$

$$\mathcal{F}_s[g(x)]\equiv\hat{g}(k)=\int_0^\infty \mathrm{d}t e^{-ikx}g(x). \tag{6}$$

Applying a Fourier–Laplace transforms to the above, we find:

$$\hat{\tilde{\wp}}_r(k,s|x_0,y_0)=\frac{\hat{\tilde{\wp}}_0(k,s+r|x_0,y_0)}{1-r\hat{\tilde{\wp}}_0(k,s+r|y_0)}. \tag{7}$$

This expresses the marginalized propagator of the observable variable x under resetting of the non-observable y to the corresponding propagator without resetting. Note that only the numerator is conditioned on both initial conditions, whereas the term in the denominator should be taken with $x_0=0$ as a consequence of the homogeneity assumption. Propagators of this form were recently studied in detail for fractional Brownian motion in [23]. Here, we use equation (7) to derive a hierarchy of moments from which exact expressions for the coefficients governing late-time scaling is provided. We later extend these results to also allow refractory periods of arbitrary durations after each reset.

2.1. Hierarchy of moments

Inverting the above solution in equation (7) can be exactly arduous in many cases, as the marginalized propagators even in simple coupled systems have complex Fourier–Laplace transforms. To make further progress, we derive from it a general expression for the moments of the process x_t. First, note that moments can be computed from Fourier transforms of the probability density as:

$$\langle x^n|x_0,y_0\rangle_t=\frac{\partial^n}{\partial(ik)^n}\hat{\wp}_r(k,t|x_0,y_0)\bigg|_{k=0}. \tag{8}$$

As we have the Fourier–Laplace transform, we will in our case find:

$$\widetilde{\langle x^n|x_0,y_0\rangle}_s=\frac{\partial^n}{\partial(ik)^n}\hat{\tilde{\wp}}_r(k,s|x_0,y_0)\bigg|_{k=0}, \tag{9}$$

J. Stat. Mech. (2024) 033210

where $\widetilde{\langle x^n|x_0,y_0\rangle}_s = \mathcal{L}_{t\to s}\left[\langle x^n|x_0,y_0\rangle_t\right]$ denotes Laplace transforms. To obtain expressions for the moments from equation (7), we first re-write it as:

$$\hat{\tilde{\wp}}_r\left(k,s|x_0,y_0\right)\left[1-r\hat{\tilde{\wp}}_0\left(k,s+r|y_0\right)\right]=\hat{\tilde{\wp}}_0\left(k,s+r|x_0,y_0\right) \tag{10}$$

simply to avoid having to deal with quotients. Using the generalized product rule for higher-order derivatives, we have:

$$\begin{aligned}\frac{\partial^n}{\partial\left(ik\right)^n}\hat{\tilde{\wp}}_0\left(k,s+r|x_0,y_0\right)=&\sum_{\ell=0}^{n}\binom{n}{\ell}\frac{\partial^{(n-\ell)}}{\partial\left(ik\right)^{(n-\ell)}}\hat{\tilde{\wp}}_r\left(k,s|x_0,y_0\right)\\&\times\frac{\partial^\ell}{\partial\left(ik\right)^\ell}\left[1-r\hat{\tilde{\wp}}_0\left(k,s+r|y_0\right)\right].\end{aligned} \tag{11}$$

Setting $k=0$ and using the expression for the moments, we have:

$$\widetilde{\langle x^n|x_0,y_0\rangle}^{(0)}_{s+r}=\sum_{\ell=0}^{n}\binom{n}{\ell}\widetilde{\langle x^{n-\ell}|x_0,y_0\rangle}_s\left[\delta_{\ell,0}-r\widetilde{\langle x^\ell|y_0\rangle}^{(0)}_{s+r}\right], \tag{12}$$

where the superscript (0) denotes moments for the underlying process with $r=0$. Rearranging gives:

$$\widetilde{\langle x^n|x_0,y_0\rangle}_s=\frac{s+r}{s}\widetilde{\langle x^n|x_0,y_0\rangle}^{(0)}_{s+r}+\frac{s+r}{s}\left[r\sum_{\ell=1}^{n}\binom{n}{\ell}\widetilde{\langle x^{n-\ell}|x_0,y_0\rangle}_s\widetilde{\langle x^\ell|y_0\rangle}^{(0)}_{s+r}\right]. \tag{13}$$

This recursive relation can be used to iteratively construct any moment of the process x_t given the lower-order moments and the moments of the $r=0$ case, which are assumed to be known. We emphasize that this result can be useful when the Fourier–Laplace transforms of the propagator itself is hard to obtain, whereas if $\hat{\tilde{p}}_0(k,s|x_0,y_0)$ is known one can simply expand equation (7) in powers of k to identify the moments. We also note that when $r=0$, the above equation reduces to $\langle x^n|x_0,y_0\rangle_s=\langle x^n|x_0,y_0\rangle^{(0)}_s$ as it should.

3. Transport processes: crossover from anomalous to normal diffusion

For transport processes, the relevant physical variables are often the position x_t and velocity v_t of a particle, satisfying $\dot{x}_t=v_t$. Here, we consider the effect of velocity resetting on spatial transport by using equation (13). This is of relevance to a wide range of systemsfor example, for particles with inelastic collisions with an environment or substrate, or in foraging processes where animals intermittently stop (e.g., to collect nutrients or scout for predators) before re-starting their motion from zero velocity but unchanged position. Starting from the hierarchy in equation (13), we derive general expressions for the effective drift and diffusivity and consider in more detail the case where the underlying process shows anomalous diffusion.

J. Stat. Mech. (2024) 033210

3.1. Effective transport coefficients

To characterize transport, we are interested in the first two spatial moments:

$$\widetilde{\langle x|x_0,v_0\rangle}_s = \frac{s+r}{s}\left[\widetilde{\langle x|x_0,v_0\rangle}^{(0)}_{s+r} + \frac{r}{s}\widetilde{\langle x|v_0\rangle}^{(0)}_{s+r}\right], \tag{14}$$

$$\begin{aligned}\widetilde{\langle x^2|x_0,v_0\rangle}_s = &\frac{s+r}{s}\widetilde{\langle x^2|x_0,v_0\rangle}^{(0)}_{s+r} + \frac{s+r}{s}\frac{r}{s}\widetilde{\langle x^2|v_0\rangle}^{(0)}_{s+r} \\ &+ \frac{s+r}{s}\left[2r\widetilde{\langle x|x_0,v_0\rangle}_s\widetilde{\langle x|v_0\rangle}^{(0)}_{s+r}\right],\end{aligned} \tag{15}$$

which contain information regarding the effective drift and dispersion of the spatial variable. Without any loss of generality, let us consider $x_0=0$. Then, the first moment can be written compactly as:

$$\widetilde{\langle x|0,v_0\rangle}_s = \left(\frac{s+r}{s}\right)^2 \widetilde{\langle x|0,v_0\rangle}^{(0)}_{s+r}. \tag{16}$$

At late times, corresponding to small values of s, the s^{-2} pole dominates, giving rise to a linear growth in time. The inverse Laplace transform can be calculated in terms of residues as:

$$\begin{aligned}\langle x|0,v_0\rangle_t &= \mathcal{L}^{-1}_{s\to t}\left\{\left(\frac{s+r}{s}\right)^2 \widetilde{\langle x|0,v_0\rangle}^{(0)}_{s+r}\right\} \\ &= \sum_{\text{poles }\{s_i\}} \text{Res}_i\left[\left(\frac{s+r}{s}\right)^2 \widetilde{\langle x|0,v_0\rangle}^{(0)}_{s+r} e^{st}\right],\end{aligned} \tag{17}$$

where the poles $\{s_i\}$ are those of equation (16). The poles at non-zero values of s give rise to exponentially decaying terms. Hence, the late-time behavior is extracted from the pole at zero, in which case the residue reads:

$$\langle x|0,v_0\rangle_t = \lim_{s\to 0}\partial_s\left[(s+r)^2\widetilde{\langle x|0,v_0\rangle}^{(0)}_{s+r}e^{st}\right] = r^2\widetilde{\langle x|0,v_0\rangle}^{(0)}_{r}\, t + \ldots \tag{18}$$

where the terms $+\ldots$ represent terms that are either approaching a constant or vanishing at late times. The effective drift at late times is then calculated as:

$$V_{\text{eff}} \equiv \lim_{t\to\infty}\frac{\langle x|0,v_0\rangle_t}{t} = r^2\widetilde{\langle x|0,v_0\rangle}^{(0)}_{r}. \tag{19}$$

Hence, velocity resetting to a non-zero value of velocity v_0, which typically results in non-zero $\langle x|0,v_0\rangle^{(0)}_t$, will result in a drift at late times, as is expected[2]. This can be seen

[2] It should be noted that one may in principle reset velocity to a non-zero value v_0 and yet obtain a vanishing mean $\langle x|0,v_0\rangle^{(0)}_t$. For example, in the presence on a constant external drift one could reset to a velocity that exactly opposes the drift.

J. Stat. Mech. (2024) 033210

as a rectification effect due to velocity resetting. The physical intuition of equation (19) is obtained by noting that the late-time behavior of the mean position can be written:

$$\langle x|0,v_0\rangle_t \simeq V_{\rm eff}t = (rt)\int {\rm d}t r{\rm e}^{-rt}\langle x|0,v_0\rangle_t^{(0)} \tag{20}$$

which is nothing but the mean number of resets $\overline{n}=rt$ in time t, times the mean step length during an inter-reset epoch.

In the remainder of this section, we consider for simplicity symmetric processes with vanishing odd moments such that no drift is present $V_{\rm eff}=0$, and set $v_0=0$. Proceeding similarly to the effective drift, we can derive an expression for the effective diffusivity. The second moment in the Laplace space reads:

$$\widetilde{\langle x^2|0,0\rangle}_s = \left(\frac{s+r}{s}\right)^2 \widetilde{\langle x^2|0,0\rangle}^{(0)}_{s+r}. \tag{21}$$

By the same logic, the s^{-2} pole gives rise to a linearly growing mean-squared-displacement. Again, the real-time mean squared displacement can be expressed as a sum over poles s_i of equation (21):

$$\begin{aligned}\langle x^2|0,0\rangle_t &= \mathcal{L}^{-1}_{s\to t}\left\{\left(\frac{s+r}{s}\right)^2 \widetilde{\langle x^2|0,0\rangle}^{(0)}_{s+r}\right\}\\ &= \sum_{\text{poles }\{s_i\}} {\rm Res}_i\left[\left(\frac{s+r}{s}\right)^2 \widetilde{\langle x^2|0,0\rangle}^{(0)}_{s+r} e^{st}\right].\end{aligned} \tag{22}$$

The dominant late-time behavior once again comes from the second-order pole at $s=0$, resulting in:

$$\langle x^2|0,0\rangle_t = \lim_{s\to 0}\partial_s\left[(s+r)^2\,\widetilde{\langle x^2|0,0\rangle}^{(0)}_{s+r}e^{st}\right] = r^2\widetilde{\langle x^2|0,0\rangle}^{(0)}_{r}\,t+\ldots. \tag{23}$$

Hence, the effective diffusivity can be calculated as:

$$D_{\rm eff}\equiv\lim_{t\to\infty}\frac{\langle x^2|0,0\rangle_t}{2t} = \frac{r^2}{2}\widetilde{\langle x^2|0,0\rangle}^{(0)}_{r}. \tag{24}$$

As for the effective drift, a natural physical interpretation of this in terms of the asymptotic behavior of the mean squared displacement can be obtained by noticing that:

$$\langle x^2|0,0\rangle_t \simeq 2D_{\rm eff}t = rt\int_0^\infty {\rm d}t r{\rm e}^{-rt}\langle x^2|0,0\rangle_t^{(0)} \tag{25}$$

which is the mean number of resets $\overline{n}$ times the mean growth of the second moment during an inter-reset epoch. We focus on the generality of this result, as long as the system considered is spatially homogeneous, and the full renewal structure of equation (1) is satisfied, the process under velocity resets will display normal diffusion with the above

J. Stat. Mech. (2024) 033210

effective diffusivity, even if the reset-free system shows anomalous diffusion. We discuss this further in later sections.

Underdamped Brownian motion: as a simple application of the above formula, we consider velocity resetting for an underdamped Brownian particle. This can be viewed as a minimal model for a particle moving through a complex environment, where intermittently the particle collides with the environment and loses its momentum [42]. The particle obeys the coupled equations:

$$\mathrm{d}x_\tau = v_\tau \mathrm{d}t, \tag{26}$$

$$\mathrm{d}v_\tau = -\gamma v_\tau \mathrm{d}t + \sqrt{2k_B T\gamma}\mathrm{d}W, \tag{27}$$

where $\mathrm{d}W$ is an increment in the Wiener process and γ the friction coefficient. Here, we have set mass to unity. The marginalized position distribution reads [17]:

$$\wp_0(x,t|x_0,v_0) = \frac{1}{\sqrt{2\pi\,\Sigma_t^2}}\exp\left(-\frac{(x-\langle x_t\rangle)^2}{2\Sigma_t^2}\right), \tag{28}$$

where the variance and mean of the density reads:

$$\Sigma_t^2 = D_0\tau_\gamma\left(\frac{2t}{\tau_\gamma} + 4\mathrm{e}^{-t/\tau_\gamma} - \mathrm{e}^{-2t/\tau_\gamma} - 3\right), \tag{29}$$

$$\langle x_t\rangle = x_0 + v_0\tau_\gamma\left(1-\mathrm{e}^{-t/\tau_\gamma}\right), \tag{30}$$

with $\tau_\gamma = 1/\gamma$ being the inertial timescale and $D_0 = k_BT/\gamma$. From this, one can easily calculate the second moment in the Laplace space, resulting in:

$$\widetilde{\langle x^2|0,0\rangle}_s^{(0)} = -\frac{3D_0}{\gamma s} + \frac{4D_0}{\gamma(\gamma+s)} - \frac{D_0}{\gamma(2\gamma+s)} + \frac{2D_0}{s^2}, \tag{31}$$

where we set $x_0 = v_0 = 0$, so that $V_{\mathrm{eff}} = 0$. Using equation (24), one immediately finds:

$$\frac{D_{\mathrm{eff}}}{D_0} = \left(1+\zeta\,\frac{3+\zeta}{2}\right)^{-1}. \tag{32}$$

Here, we introduce the dimensionless variable $\zeta = r/\gamma$. As expected, $D_{\mathrm{eff}} = D_0$ is obtained when $\zeta = 0$, which can be achieved either by $r = 0$ or in the high-friction limit $\gamma \to \infty$. The latter case highlights the fact that for Brownian particles, a non-trivial effective diffusivity only occurs in the presence of inertial effects, whereby the particle must accelerate after each reset. We also observed that velocity resetting suppresses spatial transport, and $D_{\mathrm{eff}} = 0$ as $r \to \infty$. This is verified using numerical simulations in figure 2.

3.2. When the underlying process is anomalous

The above results have interesting implications for transport processes in (x, v) that would be anomalous in the absence of resetting. Anomalous diffusion processes with

J. Stat. Mech. (2024) 033210

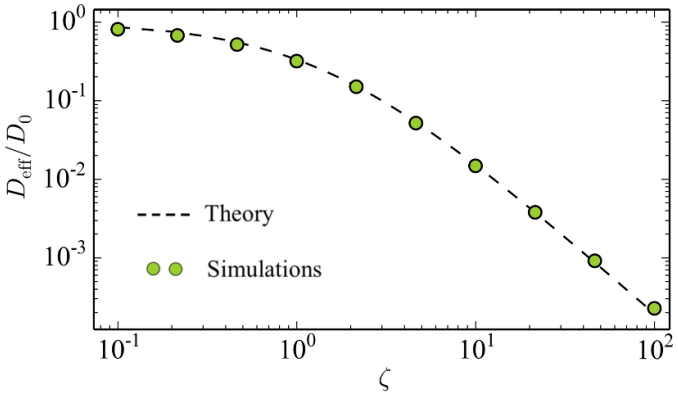

Figure 2. Effective diffusivity for an underdamped Brownian motion undergoing velocity resetting, as a function of re-scaled resetting rate $\zeta = r/\gamma$. Dashed black lines show exact theory (equation (32)), whereas points show simulated data, using $D_0 = \gamma = 1$.

resetting have been studied recently for overdamped systems in the context of ergodicity breaking and restoration [43–46]. Here, we investigate the effects of velocity resetting in underdamped anomalous systems.

For anomalous diffusion processes, the underlying process satisfies in the simplest case:

$$\langle x^2|0,0\rangle_t^{(0)} = D_0 t^\alpha, \tag{33}$$

with diffusion exponent α taking any positive real value. Such processes are present in a wide range of systems, with classical examples being the transport of Brownian particles in complex environments, such as fractals or media with power-law friction [47–53]. Anomalous diffusion has also been observed in granular systems, such as in the velocity profile of fluid-driven silo discharge [54], in granular gases near a shear instability [55], and in the height fluctuations in graphene [56]. In such cases, one often expects subdiffusive processes $\alpha < 1$, whereas there are also cases where superdiffusion with $\alpha > 1$ occurs, such as in Lévy flights, random acceleration processes, tracers in the turbulent flow, active particles with time-dependent self-propulsion forces, and in diffusion with density-dependent diffusivity [57–62]. For a review of theoretical models of anomalous diffusion, see, for example [63]. Although most of these studies consider particles in the overdamped limit, with no coupled variables, many models can be extended to the underdamped case and studied under the framework presented here.

The Laplace transforms in the time of equation (33) reads $\langle x^2|0,0\rangle_s^{(0)} = D_0 s^{-(1+\alpha)}\Gamma(1+\alpha)$. Using equation (21), this leads directly to:

$$\widetilde{\langle x^2|0,0\rangle}_s = \frac{D_0\Gamma(\alpha+1)(r+s)^{1-\alpha}}{s^2}. \tag{34}$$

J. Stat. Mech. (2024) 033210

Inverting gives the full time dependence of the mean-squared-displacement:

$$\langle x^2|x_0,v_0\rangle_t = (\alpha-1)\,D_0 r^{-\alpha}\left(\alpha\Gamma\left(\alpha,rt\right)-\Gamma\left(\alpha+1\right)\right) + (\alpha-1)\,\alpha D_0 r^{1-\alpha}\left(\Gamma\left(\alpha-1\right)-\Gamma\left(\alpha-1,rt\right)\right)t, \tag{35}$$

where $\Gamma(x,z)$ is the (upper) incomplete Gamma function. At early times, as resetting has not yet had time to occur, the mean-squared-displacement behaves as in the underlying system. Generally, the short-time behavior of the mean squared displacement can be obtained by looking at large values of its Laplace variable. For $s \gg r$ in equation (21) we see that $\langle x^2|0,0\rangle_s = \langle x^2|0,0\rangle_s^{(0)}$. Hence, in this case, we have $\langle x^2|0,0\rangle_t = D_0 t^\alpha$. At later times, we see that a linear growth takes over, in agreement with what we predicted more generally (see equations (23) and (24)). The effective diffusivity can be calculated either from equation (24) or directly from equation (35), yielding:

$$D_{\text{eff}} \equiv \lim_{t\to\infty}\frac{\langle x^2|0,0\rangle_t}{2t} = \frac{D_0\Gamma\left(\alpha+1\right)}{2r^{\alpha-1}}. \tag{36}$$

We see that anomalous diffusion processes with diffusion exponent α become normal under velocity resetting, with an effective diffusion coefficient scaling with resetting rate as $D_{\text{eff}} \sim r^{1-\alpha}$. For superdiffusive processes, the effective diffusivity decreases as a function of resetting rate, whereas for subdiffusive processes it grows with increasing resetting rate. The fact that subdiffusive processes can enhance their diffusivity by resetting originates in the full renewal structure of equation (1). Since subdiffusion often occurs for processes that slow down substantially over time, such as for single-file diffusion [64, 65], restarting to a state of higher motility can be beneficial. The crossover time t_* where the linear growth starts to dominate over the anomalous growth can be identified by matching the late-time regime with the effective diffusivity given by equation (36) with the early-time growth $D_0 t^\alpha$, resulting in:

$$t_* = \left[\frac{\Gamma\left(\alpha+1\right)}{2}\right]^{\frac{1}{\alpha-1}} r^{-1}. \tag{37}$$

Since the resetting timescale r^{-1} determines when the mean squared displacement should cross over to linear growth, this proportionality is sensible.

Random acceleration process: a concrete example of the above could be the random acceleration process [59]

$$\dot{x} = v, \tag{38}$$

$$\dot{v} = \sqrt{2}\eta\left(t\right), \tag{39}$$

where $\eta(t)$ is a Gaussian white noise with correlator $\langle\eta(t_1)\eta(t_2)\rangle = \delta(t_1-t_2)$, and where we set the noise strength to unity for simplicity. The marginalized process $\wp_0(x,t|x_0,v_0)$ is known to have a Gaussian propagator [18, 59]

$$\wp_0\left(x,t|0,0\right) = \sqrt{\frac{3}{4\pi t^3}}\exp\left(-\frac{3}{4t^3}x^2\right), \tag{40}$$

J. Stat. Mech. (2024) 033210

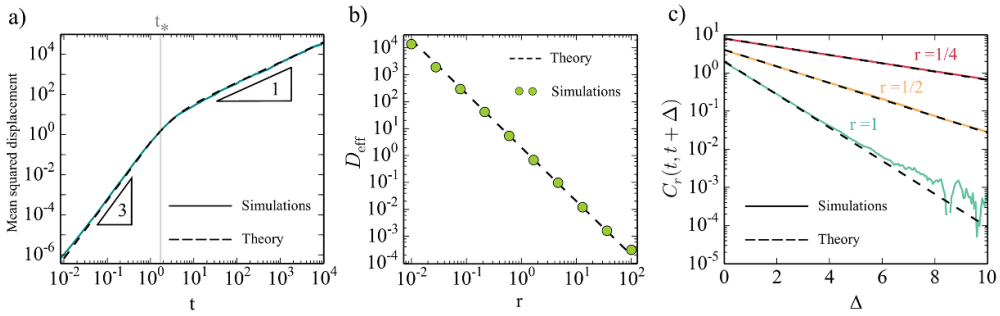

Figure 3. Comparisons of theory (dashed black lines) and simulated data for a random acceleration process. (a) Mean squared displacement shows a clear crossover from anomalous $\alpha = 3$ diffusion to normal diffusion with $\alpha = 1$ at times larger than the crossover time t_*(gray vertical line). (b) Effective diffusivity at late times scales as $D_{\rm eff} \sim r^{-2}$, as predicted by equation (36). (c) Velocity auto-correlation functions showing exponential tempering. Solid colored lines are simulations, while black dashed line corresponds to equation (44). Resetting rate is set to unity unless stated otherwise.

with a mean squared displacement that grows as a cubic in time $\langle x^2|0,0\rangle_t^{(0)} = \frac{2}{3}t^3$, that is $\alpha = 3$ and $D_0 = 2/3$ in the above calculation. The effective diffusivity after resetting reads $D_{\rm eff} = 2/r^2$, with a crossover time $t_* = \sqrt{3}/r$. This result was also reported in [23] obtained by other methods. Here, the full mean-squared-displacement can easily be obtained from equation (35), which we show in figure 3(a), where a clear crossover from anomalous $\alpha = 3$ to normal $\alpha = 1$ is seen. The predicted $D_{\rm eff} \sim r^{-2}$ scaling also matches perfectly with simulated data as seen in figure 3(b).

3.3. Tempered correlation functions

The emergence of normal diffusion independently of the anomalous nature of the underlying process can be understood as a consequence of resetting-induced tempering of the velocity auto-correlation functions. It is well known that systems with exponential (or sufficiently strong power law) cutoffs display a crossover from anomalous to normal diffusion at late times [66].

For transport processes, the position is coupled to velocity simply through $\dot{x} = v$, implying that the mean squared displacement in general comes from the temporal behavior of the velocity correlation functions:

$$\langle (x - x_0)^2 \rangle_t = 2 \int_0^t \mathrm{d}\tau_2 \int_0^{\tau_2} \mathrm{d}\tau_1 C_r(\tau_1, \tau_2), \tag{41}$$

where we introduced $C_r(\tau_1, \tau_2) = \langle v_{\tau_1} v_{\tau_2} \rangle$. We will by $C_0(\tau_1, \tau_2)$ denote the velocity auto-correlations in the absence of resetting. For correlations that decay sufficiently fast, the system exhibits normal diffusion and the above equation can be turned into a Green–Kubo relation for the diffusion coefficient. If the correlation functions decay too slowly, or even grow in time, one expects anomalous diffusion.

J. Stat. Mech. (2024) 033210

Similarly, to the probability density, correlation functions are known to satisfy a renewal equation of the type [6, 67]:

$$C_r(t_1,t_2) = \mathrm{e}^{-rt_2}C_0(t_1,t_2) + r\mathrm{e}^{-r(t_2-t_1)}\int_0^{t_1}\mathrm{d}\tau\mathrm{e}^{-r\tau}C_0(\tau,t_2-t_1+\tau). \tag{42}$$

Here we rely on the assumption that the position is coupled to the velocity, but not vice versa, allowing a simple renewal equation for the velocity correlations. This is normal for most models of Brownian motion and has been utilized in the past where considering underdamped Brownian motion under partial resetting of position alone [17]. We already show that the inclusion of resetting tempers the correlations by including an exponential cutoff at a characteristic time r^{-1} already in the first term.

Returning again to a concrete example where the underlying process is anomalous of the type equation (33), we consider correlation functions of the form:

$$C_0(t_1,t_2) = \frac{\alpha(\alpha-1)D_0}{2}\min\{t_1,t_2\}^{\alpha-2}. \tag{43}$$

This correlation function is chosen so that by applying equation (41) it gives rise to a mean squared displacement growing anomalously in time with exponent α. Under resetting, the new correlator equation (42) reads:

$$C_r(t_1,t_2) = \frac{\alpha(\alpha-1)D_0}{2}\mathrm{e}^{-r(t_2-t_1)}\left(r^{2-\alpha}\left(\Gamma(\alpha-1)-\Gamma(\alpha-1,rt_1)\right)+t_1^{\alpha-2}\mathrm{e}^{-rt_1}\right),$$

where we assumed $t_2 \geqslant t_1$. To clearly see the tempering, consider $C_r(t,t+\Delta)$ with $\Delta \geqslant 0$ a lag variable. For $t \gg r^{-1}$ we then find:

$$C_r(t,t+\Delta) \simeq \frac{\Gamma(\alpha+1)D_0 r^{2-\alpha}}{2}\mathrm{e}^{-r\Delta}, \tag{44}$$

which shows a clear cutoff scale r^{-1}. This exponential behavior is shown for the random acceleration process in figure 3(c), where, normally, the velocity correlations obey equation (43) with $\alpha = 3$.

3.4. The effect of real-time crossovers

As a final example, we consider the case where the underlying system has a crossover from one dynamical regime to another at a crossover time t_c. We assume

$$\langle x^2\rangle_t^{(0)} = 2D_\alpha t^\alpha\theta(t_c-t) + 2D_\beta t^\beta\theta(t-t_c). \tag{45}$$

The effective diffusivity can again be calculated from equation (24), resulting in

$$D_{\mathrm{eff}}(r) = D_\alpha r^{1-\alpha}\gamma(\alpha+1,rt_c) + D_\beta r^{1-\beta}\Gamma(\beta+1,rt_c), \tag{46}$$

where $\Gamma(\cdot)$ and $\gamma(\cdot)$ are the upper and lower incomplete Gamma functions respectively. We note that while $\gamma(a,z)$ vanishes as $z\to 0$, $\Gamma(a,z)$ simply approaches $\Gamma(a)$ in this

J. Stat. Mech. (2024) 033210

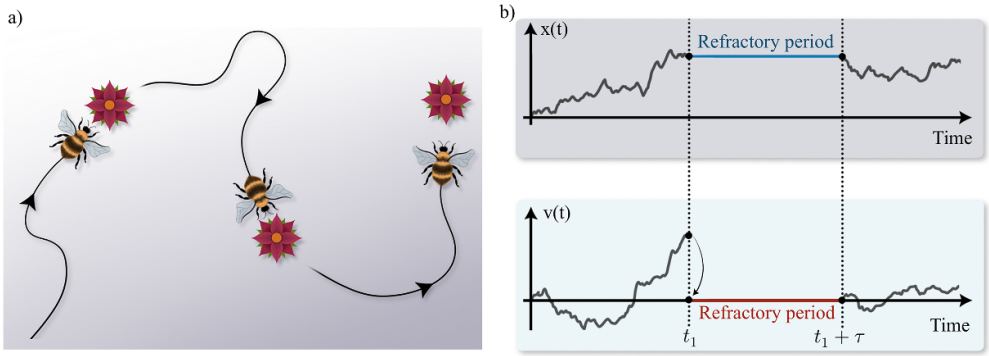

Figure 4. Sketch of the system considered in this paper. (a) Typical dynamics of a forager consists of exploration phases interrupted by refractory periods of no motion. (b) Sketch of one dimension time-series for position and velocity, showing a refractory period of duration τ following a resetting at time t_1. Here we assume that velocity is reset to zero, so that no motion occurs during the refractory period.

limit. A converse behavior holds for $z \to \infty$. Hence, the incomplete gamma functions give more or less weight to the two scaling behaviors depending on the value of the resetting rate. In particular, the effective diffusivity changes the scaling behavior as a function of resetting rate r at a crossover value $r_c = t_c^{-1}$. In the case $r \ll t_c^{-1}$, the system resets so rarely that the late-time dynamical regime can always be explored, and $D_{\text{eff}}(r) \sim r^{1-\beta}$. Similarly, when $r \gg t_c^{-1}$ typical trajectories only explore the first dynamical regime, and $D_{\text{eff}}(r) \sim r^{1-\alpha}$.

The underdamped Brownian particle described by equations (26) and (27) yet again serves as a good example for the case with a crossover. In this case, it is known that for a particle initially at rest, the short-time mean squared displacement has a leading-order cubic behavior [68]

$$\langle x^2 \rangle_t^{(0)} = \frac{4\gamma^2 D_0}{3} t^3 + \mathcal{O}\left(t^4\right), \tag{47}$$

while at late times it crosses over to normal diffusion $\langle x^2 \rangle_t^{(0)} \sim t$. Hence, we expect an effective diffusivity that is initially constant before decaying as r^{-2}. This is indeed what is observed in figure 2, or equivalent in equation (32).

4. Effects of refractory periods

In the case of inertial foragers that perform stop-and-go locomotion, velocity resets to $v_0 = 0$ are often followed by inactive periods (see figure 4). In the context of resetting, such idle times after the resetting events are referred to as refractory times [69, 70]. In overdamped systems with a single degree of freedom, anomalous diffusion behavior has been observed for particular choices of refractory and inter-reset statistics [71]. In this section we include the effect of such refractory times in underdamped systems and show how normal Poissonian resets of velocity can also lead to anomalous diffusion.

J. Stat. Mech. (2024) 033210

4.1. Exact propagator

For the case of velocity resetting without refractory times, we start by investigating the renewal equation. The first renewal equation for the propagator can be written as follows:

$$\begin{aligned} p_r\left(x,v,t|x_0,v_0\right) &= \mathrm{e}^{-rt}p_0\left(x,v,t|x_0,v_0\right) \\ &+ r\int_0^t \mathrm{d}t_1 \mathrm{e}^{-rt_1}\int_0^{t-t_1}\mathrm{d}\tau W\left(\tau\right)\int \mathrm{d}y\mathrm{d}u p_0\left(y,u,t_1|x_0,v_0\right)p_r\left(x,v,t-t_1-\tau|y,v_0\right) \\ &+ r\int_0^t \mathrm{d}t_1 \mathrm{e}^{-rt_1}\int_{t-t_1}^{\infty}\mathrm{d}\tau W\left(\tau\right)\int \mathrm{d}y\mathrm{d}u p_0\left(y,u,t_1|x_0,v_0\right)\delta\left(v-v_0\right)\delta\left(x-y\right). \end{aligned} \tag{48}$$

Here, the first two terms have the same interpretation as before, corresponding respectively to paths without resets and paths with resets. The only difference is the inclusion of a refractory time τ after the first reset event. The third term corresponds to paths that at time t end in the refractory phase.

As before, we will assume spatial homogeneity, which means we can do so without loss of generality set $x_0 = 0$. To ease the notation, as before, we suppress this from the propagator so that $p_i(x,v,t|x_0=0,v_0) = p_i(x,v,t|v_0)$, with $i = r,0$. Integrating the above initial renewal equation over velocity v, we find the position distribution:

$$\begin{aligned} \wp_r\left(x,t|v_0\right) &= \mathrm{e}^{-rt}\wp_0\left(x,t|v_0\right) \\ &+ r\int_0^t \mathrm{d}t_1 \mathrm{e}^{-rt_1}\int_0^{t-t_1}\mathrm{d}\tau W\left(\tau\right)\int \mathrm{d}y\wp_0\left(y,t_1|v_0\right)\wp_r\left(x,t-t_1-\tau|y,v_0\right) \\ &+ r\int_0^t \mathrm{d}t_1 \mathrm{e}^{-rt_1}\int_{t-t_1}^{\infty}\mathrm{d}\tau W\left(\tau\right)\wp_0\left(x,t_1|v_0\right). \end{aligned} \tag{49}$$

Invoking spatial homogeneity, we write $\wp_r(x,t-t_1-\tau|y,v_0) = \wp_r(x-y,t-t_1-\tau|v_0)$. Taking a Fourier transform in space, we obtain:

$$\begin{aligned} \hat{\wp}_r\left(k,t|v_0\right) &= \mathrm{e}^{-rt}\hat{\wp}_0\left(k,t|v_0\right) \\ &+ r\int_0^t \mathrm{d}t_1 \mathrm{e}^{-rt_1}\hat{\wp}_0\left(k,t_1|v_0\right)\int_0^{t-t_1}\mathrm{d}\tau W\left(\tau\right)\hat{\wp}_r\left(k,t-t_1-\tau|v_0\right) \\ &+ r\int_0^t \mathrm{d}t_1 \mathrm{e}^{-rt_1}\hat{\wp}_0\left(k,t_1|v_0\right)\int_{t-t_1}^{\infty}\mathrm{d}\tau W\left(\tau\right). \end{aligned} \tag{50}$$

Laplace transforming equation (50) results in:

$$\begin{aligned} \hat{\tilde{\wp}}_r\left(k,s|v_0\right) &= \hat{\tilde{\wp}}_0\left(k,s+r|v_0\right) + r\tilde{W}\left(s\right)\hat{\tilde{\wp}}_0\left(k,s+r|v_0\right)\hat{\tilde{\wp}}_r\left(k,s|v_0\right) \\ &+ r\frac{\hat{\tilde{\wp}}_0\left(k,s+r|v_0\right)}{s}\left[1-\tilde{W}\left(s\right)\right]. \end{aligned} \tag{51}$$

Solving for the propagator in the presence of resetting, we get the closed form expression:

$$\hat{\tilde{\wp}}_r\left(k,s|v_0\right) = \frac{\hat{\tilde{\wp}}_0\left(k,s+r|v_0\right)}{1-r\tilde{W}\left(s\right)\hat{\tilde{\wp}}_0\left(k,s+r|v_0\right)}\left(1-\frac{r}{s}\left[1-\tilde{W}\left(s\right)\right]\right). \tag{52}$$

J. Stat. Mech. (2024) 033210

This gives an exact expression for the spatial propagator for any distribution of refractory times. One can indeed verify that the propagator is normalized $\hat{\tilde{\varphi}}_r(0,s|v_0)=1/s$. Furthermore, in the case without any refractory period $W(\tau)=\delta(\tau)$, we recover previous expressions for the propagator under velocity resets.

If one cares only about late-time dynamical behavior, one may naively expect that this reduces to a simple continuous time random walk (CTRW). In this case, the propagator in the Fourier–Laplace space is given by the famous Montroll–Weiss formula, which relates the propagator to the distribution of jump lengths and the distribution of the waiting times in between each jump [72]. The classical Montroll–Weiss theory assumes independent jump lengths and waiting times, although extensions to correlated cases have been considered [73]. In the present case, the waiting time is given by the combination $t_E+\tau$, with t_E the exploration time and τ the duration of the refractory phase. The jump length, however, is determined both by the underlying propagator in the exploration phase and the duration of the exploration phase. Hence, the jump lengths depend only on the time t_E of the exploration phase and not on the duration of the refractory times. Therefore, velocity resetting with refractory times can be seen as a form of CTRW with a particular correlation between the jump lengths and the waiting times. Of course, another strong contrast to the CTRW case is that the dynamics studied here is fully time-resolved and does not perform sudden discrete jumps.

4.2. Mean squared displacement

The moments of position can be obtained from equation (52) by differentiation as before, through equation (8). Assuming that we are dealing with a process where the first moment always vanishes, which is, typically, the case if $v_0=0$, we can proceed as in earlier sections to find:

$$\widetilde{\langle x^2|0,0\rangle}_s=\widetilde{\langle x^2|0,0\rangle}^{(0)}_{s+r}\frac{1+\frac{r}{s}\left[1-\tilde{W}(s)\right]}{\left[1-\frac{r\tilde{W}(s)}{s+r}\right]^2}. \tag{53}$$

We consider two scenarios next.

4.2.1. Mean refractory period is finite ($\langle\tau\rangle<\infty$). As shown before, the late-time dynamics can be obtained by considering the small-s limit of the Laplace transformed mean squared displacement in equation (53). For small s, we can approximate $\tilde{W}(s)=1-s\langle\tau\rangle+\ldots$, in which case, the dominant singularity of the MSD is s^{-2}:

$$\widetilde{\langle x^2|0,0\rangle}_s=\frac{r^2\widetilde{\langle x^2|0,0\rangle}^{(0)}_r}{s^2\left(1+r\langle\tau\rangle\right)}. \tag{54}$$

Hence the diffusion is normal, with an effective diffusion coefficient

$$D_{\rm eff}=\lim_{t\to\infty}\frac{\langle x^2(t)|0,0\rangle}{2t}=\frac{r^2\widetilde{\langle x^2|0,0\rangle}^{(0)}_r}{2+2r\langle\tau\rangle}. \tag{55}$$

J. Stat. Mech. (2024) 033210

We see that refractory times suppress the effective diffusion, and when $\langle\tau\rangle = 0$ we recover previous results.

4.2.2. Mean refractory period is infinite ($\langle\tau\rangle = \infty$). If the mean refractory time diverges due to power-law distributed refractory periods $W(\tau) \sim 1/(\tau^{1+\alpha})$ with $\tilde{W}(s) \sim 1 - as^{\alpha}$, for some constant a and $\alpha \in (0,1)$, we instead find the small-s behavior:

$$\widetilde{\langle x^2|0,0\rangle}_s = \frac{r\widetilde{\langle x^2|0,0\rangle}_r^{(0)}}{as^{1+\alpha}}. \tag{56}$$

In this case, the MSD in real-time reads:

$$\langle x^2(t)\rangle \simeq \frac{r\widetilde{\langle x^2|0,0\rangle}_r^{(0)}}{a} t^{\alpha}, \tag{57}$$

with $\simeq$ denoting equality at late times. Hence, the particle will exhibit anomalous diffusion of the sub-diffusive type independently of its underlying dynamics, simply as a consequence of the long refractory periods.

5. Conclusion and outlook

In this paper, we study stochastic resetting in coupled systems, with a particular focus on position and velocity. A general result is derived for the propagator for an observable variable under the indirect effect of resetting of a hidden variable. From this finding, we derive a general recursive equation for the moments, from which one can in principle fully characterize the marginalized process. We apply the proposed framework to transport processes of inertial particles where the velocity undergoes resetting, and show that generically the late-time dynamics shows normal diffusion even if the reset-free system is anomalous. We attribute this outcome to the tempering effect stochastic resetting has on velocity auto-correlation functions. We derive compact expressions for the effective drift and diffusivity coefficients. When a temporal crossover between two dynamical regimes exists in the underlying dynamics, this translates into a crossover as a function of the resetting rate in the effective diffusivity, where different scaling behaviors are observed. We test the validity of our predictions in the cases of underdamped Brownian motion and for the random acceleration process, both showing excellent agreement with simulated data. Extensions to the case where refractory periods are included after each reset are also considered, in which case resetting-induced anomalous diffusion can be observed.

The main results of this paper are based on two crucial assumptions. The first is the homogeneity in the variable x that is not reset, and the second is the full renewal structure represented by equation (1). Extensions of the results presented here to account for either spatial heterogeneity or, for example, non-renewal reset structures such as in [41] would be very interesting, thus highlighting anomalous diffusion processes with velocity resets in systems with quenched or annealed disorder. Generalizations to more complex

J. Stat. Mech. (2024) 033210

types of resetting, such as proportional resetting [42] or non-Poissonian waiting times, can also be considered.

Finally, it would also be interesting to investigate resetting in coupled systems from a thermodynamic perspective. Recently, much effort has been put into understanding the stochastic thermodynamics of resetting, with both entropy production and work having been considered [12–14]. However, in the present model, the observable variable is not the one undergoing resets. Hence, it would be interesting to investigate bounds on the thermodynamic cost based on partial accessible information, a topic which has gained considerable attention in the past decade [74–83].

Acknowledgments

Insightful discussions and interactions with Kevin Pierce and Deepak Gupta are gratefully acknowledged. The authors acknowledge support from the Deutsche Forschungsgemeinschaft (DFG) within the Project LO 418/29-1.

References

[1] Doering C R 2018 *Modeling Complex Systems: Stochastic Processes, Stochastic Differential Equations and Fokker-Planck Equations* (*1990 Lectures in Complex Systems*) (CRC Press) pp 3–52
[2] Van Kampen N G 1992 *Stochastic Processes in Physics and Chemistry* vol 1 (Elsevier)
[3] Risken H and Risken H 1996 *Fokker-Planck Equation* (Springer)
[4] Evans M R and Majumdar S N 2011 *Phys. Rev. Lett.* **106** 160601
[5] Evans M R and Majumdar S N 2011 *J. Phys. A: Math. Theor.* **44** 435001
[6] Evans M R, Majumdar S N and Schehr G 2020 *J. Phys. A: Math. Theor.* **53** 193001
[7] Reuveni S 2016 *Phys. Rev. Lett.* **116** 170601
[8] Pal A and Reuveni S 2017 *Phys. Rev. Lett.* **118** 030603
[9] Pal A, Kuśmierz L and Reuveni S 2020 *Phys. Rev. Res.* **2** 043174
[10] Fuchs J, Goldt S and Seifert U 2016 *Europhys. Lett.* **113** 60009
[11] Gupta D, Plata C A and Pal A 2020 *Phys. Rev. Lett.* **124** 110608
[12] Gupta D and Plata C A 2022 *New J. Phys.* **24** 113034
[13] Mori F, Olsen K S and Krishnamurthy S 2023 *Phys. Rev. Res.* **5** 023103
[14] Olsen K S, Gupta D, Mori F and Krishnamurthy S 2023 arXiv:2310.11267
[15] Olsen K S and Gupta D 2024 Thermodynamic work of partial resetting (arXiv:2401.11919)
[16] Abdoli I and Sharma A 2021 *Soft Matter* **17** 1307–16
[17] Gupta D 2019 *J. Stat. Mech.* 033212
[18] Singh P 2020 *J. Phys. A: Math. Theor.* **53** 405005
[19] Capała K and Dybiec B 2021 *J. Stat. Mech.* 083216
[20] Meylahn J M, Sabhapandit S and Touchette H 2015 *Phys. Rev.* E **92** 062148
[21] Harris R J and Touchette H 2017 *J. Phys. A: Math. Theor.* **50** 10LT01
[22] Den Hollander F, Majumdar S N, Meylahn J M and Touchette H 2019 *J. Phys. A: Math. Theor.* **52** 175001
[23] Smith N R and Majumdar S N 2022 *J. Stat. Mech.* 053212
[24] Evans M R and Majumdar S N 2018 *J. Phys. A: Math. Theor.* **51** 475003
[25] Santra I, Basu U and Sabhapandit S 2020 *J. Stat. Mech.* 113206
[26] Kumar V, Sadekar O and Basu U 2020 *Phys. Rev.* E **102** 052129
[27] Mori F, Le Doussal P, Majumdar S N and Schehr G 2020 *Phys. Rev.* E **102** 042133
[28] Olsen K S 2023 *Phys. Rev.* E **108** 044120
[29] Taylor G I 1922 *Proc. Lond. Math. Soc.* **2** 196–212
[30] Goldstein S 1951 *Q. J. Mech. Appl. Math.* **4** 129–56
[31] Lovely P S and Dahlquist F 1975 *J. Theor. Biol.* **50** 477–96
[32] Gueneau M, Majumdar S N and Schehr G 2023 arXiv:2306.09453

J. Stat. Mech. (2024) 033210

[33] Bartumeus F 2009 *Oikos* **118** 488–94
[34] Kramer D L and McLaughlin R L 2001 *Am. Zool.* **41** 137–53
[35] Stojan-Dolar M and Heymann E W 2010 *Int. J. Primatol.* **31** 677–92
[36] Wilson A D and Godin J G J 2010 *Behav. Ecol.* **21** 57–62
[37] Trouilloud W, Delisle A and Kramer D L 2004 *Animal Behav.* **67** 789–97
[38] Higham T E, Korchari P and McBrayer L D 2011 *Biol. J. Linn. Soc.* **102** 83–90
[39] Bodrova A S, Chechkin A V and Sokolov I M 2019 *Phys. Rev.* E **100** 012120
[40] Bressloff P C 2020 *J. Phys. A: Math. Theor.* **53** 275003
[41] Bodrova A S, Chechkin A V and Sokolov I M 2019 *Phys. Rev.* E **100** 012119
[42] Pierce J K 2022 arXiv:2204.07215
[43] Wang W, Cherstvy A G, Metzler R and Sokolov I M 2022 *Phys. Rev. Res.* **4** 013161
[44] Vinod D, Cherstvy A G, Metzler R and Sokolov I M 2022 *Phys. Rev.* E **106** 034137
[45] Vinod D, Cherstvy A G, Wang W, Metzler R and Sokolov I M 2022 *Phys. Rev.* E **105** L012106
[46] Liang Y, Wang W, Metzler R and Cherstvy A G 2023 *Phys. Rev.* E **108** 034113
[47] Havlin S and Ben-Avraham D 1987 *Adv. Phys.* **36** 695–798
[48] Bouchaud J P and Georges A 1990 *Phys. Rep.* **195** 127–293
[49] Ben-Avraham D and Havlin S 2000 *Diffusion and Reactions in Fractals and Disordered Systems* (Cambridge University Press)
[50] Sokolov I M 2012 *Soft Matter* **8** 9043–52
[51] Olsen K S, Flekkoy E G, Angheluta L, Campbell J M, Måløy K J and Sandnes B 2019 *New J. Phys.* **21** 063020
[52] Olsen K S and Campbell J M 2020 *Front. Phys.* **8** 83
[53] Olsen K S, Angheluta L and Flekkøy E G 2021 *Soft Matter* **17** 2151–7
[54] Morgan M L, James D W, Monloubou M, Olsen K S and Sandnes B 2021 *Phys. Rev.* E **104** 044908
[55] Brey J J and Ruiz-Montero M J 2015 *Phys. Rev.* E **92** 010201
[56] Granato E, Greb M, Elder K, Ying S and Ala-Nissila T 2022 *Phys. Rev.* B **105** L201409
[57] Dubkov A A, Spagnolo B and Uchaikin V V 2008 *Int. J. Bifurcation Chaos* **18** 2649–72
[58] Richardson L F 1926 *Proc. R. Soc.* A **110** 709–37
[59] Burkhardt T W 2014 First passage of a randomly accelerated particle *First-Passage Phenomena and Their Applications* (World Scientific) pp 21–44
[60] Hansen A, Flekkøy E G and Baldelli B 2020 *Front. Phys.* **8** 519624
[61] Babel S, Ten Hagen B and Löwen H 2014 *J. Stat. Mech.* 02011
[62] Flekkøy E G, Hansen A and Baldelli B 2021 *Front. Phys.* **9** 640560
[63] Metzler R, Jeon J H, Cherstvy A G and Barkai E 2014 *Phys. Chem. Chem. Phys.* **16** 24128–64
[64] Wei Q H, Bechinger C and Leiderer P 2000 *Science* **287** 625–7
[65] Kollmann M 2003 *Phys. Rev. Lett.* **90** 180602
[66] Molina-Garcia D, Sandev T, Safdari H, Pagnini G, Chechkin A and Metzler R 2018 *New J. Phys.* **20** 103027
[67] Majumdar S N and Oshanin G 2018 *J. Phys. A: Math. Theor.* **51** 435001
[68] Breoni D, Schmiedeberg M and Löwen H 2020 *Phys. Rev.* E **102** 062604
[69] Evans M R and Majumdar S N 2018 *J. Phys. A: Math. Theor.* **52** 01LT01
[70] García-Valladares G, Gupta D, Prados A and Plata C A 2023 arXiv:2310.19913
[71] Masó-Puigdellosas A, Campos D and Méndez V 2019 *J. Stat. Mech.* 033201
[72] Montroll E W and Weiss G H 1965 *J. Math. Phys.* **6** 167–81
[73] Liu J and Bao J D 2013 *Physica* A **392** 612–7
[74] Roldán E and Parrondo J M 2010 *Phys. Rev. Lett.* **105** 150607
[75] Amann C P, Schmiedl T and Seifert U 2010 *J. Chem. Phys.* **132** 041102
[76] Polettini M and Esposito M 2017 *Phys. Rev. Lett.* **119** 240601
[77] Bilotto P, Caprini L and Vulpiani A 2021 *Phys. Rev.* E **104** 024140
[78] Ehrich J 2021 *J. Stat. Mech.* 083214
[79] Neri I 2022 *J. Phys. A: Math. Theor.* **55** 304005
[80] Ghosal A and Bisker G 2022 *Phys. Chem. Chem. Phys.* **24** 24021–31
[81] Pietzonka P and Coghi F 2023 arXiv:2305.15392
[82] Baiesi M and Falasco G 2023 arXiv:2305.04657
[83] Ghosal A and Bisker G 2023 *J. Phys. D: Appl. Phys.* **56** 254001

J. Stat. Mech. (2024) 033210